AD-A048 316 AVCO SYSTEMS DIV WILMINGTON MASS F/G 20/4
THEORETICAL STUDY OF LEADING-EDGE BUBBLES AND LEADING-EDGE STAL--ETC(U)
DEC 77 P CRIMI DAAG29-74-C-0035
UNCLASSIFIED AVSD-00356-77-CR ARO-12221.2-E NL

| 1 OF 1 |
AD
A048316

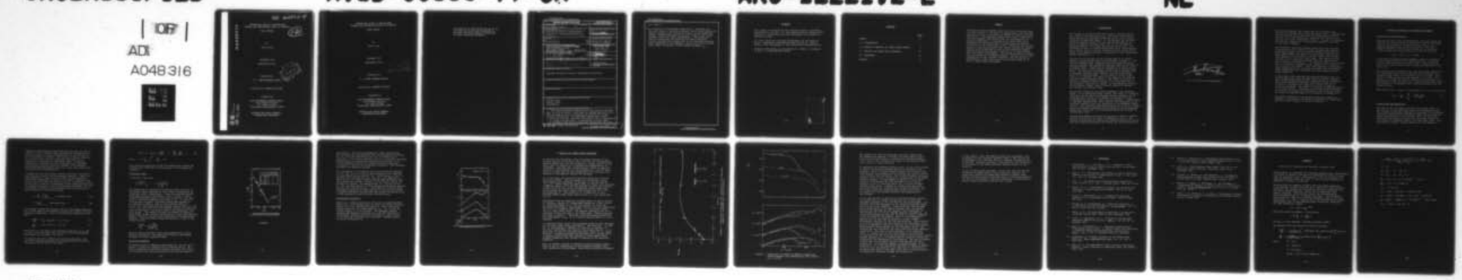

END
DATE
FILMED
2-78
DDC

ARO 12221.2-E

THEORETICAL STUDY OF LEADING-EDGE BUBBLES AND LEADING-EDGE STALL OF AIRFOILS

12

FINAL REPORT

by

Peter Crimi

December 1977

AVSD-00356-77-CR

Prepared for

U. S. ARMY RESEARCH OFFICE

Contract No. DAAG29-74-C-0035

Prepared by

AVCO GOVERNMENT PRODUCTS GROUP
Avco Systems Division
201 Lowell Street
Wilmington, Massachusetts 01887

APPROVED FOR PUBLIC RELEASE:
DISTRIBUTION UNLIMITED

THEORETICAL STUDY OF LEADING-EDGE BUBBLES AND LEADING-EDGE STALL OF AIRFOILS

FINAL REPORT

by

Peter Crimi

December 1977

AVSD-00356-77-CR

Prepared for

U. S. ARMY RESEARCH OFFICE

Contract No. DAAG29-74-C-0035

Prepared by

AVCO GOVERNMENT PRODUCTS GROUP
Avco Systems Division
201 Lowell Street
Wilmington, Massachusetts 01887

THE FINDINGS IN THIS REPORT ARE NOT TO BE CONSTRUED AS AN OFFICIAL DEPARTMENT OF THE ARMY POSITION, UNLESS SO DESIGNATED BY OTHER AUTHORIZED DOCUMENTS.

Unclassified

SECURITY CLASSIFICATION OF THIS PAGE (*When Data Entered*)

REPORT DOCUMENTATION PAGE		READ INSTRUCTIONS BEFORE COMPLETING FORM
1. REPORT NUMBER (14) AVSD-ØØ356-77-CR ✓	2. GOVT ACCESSION NO.	3. RECIPIENT'S CATALOG NUMBER
4. TITLE (*and Subtitle*) (6) Theoretical Study of Leading-Edge Bubbles and Leading-Edge Stall of Airfoils.		5. TYPE OF REPORT & PERIOD COVERED (9) Final Report. 6. PERFORMING ORG. REPORT NUMBER
7. AUTHOR(s) (10) Peter/Crimi		8. CONTRACT OR GRANT NUMBER(s) (15) DAAG29-74-C-ØØ35
9. PERFORMING ORGANIZATION NAME AND ADDRESS ~~Avco Government Products Group~~ Avco Systems Division 201 Lowell Street Wilmington, Mass. 01887 404788		10. PROGRAM ELEMENT, PROJECT, TASK AREA & WORK UNIT NUMBERS (12) 26p.
11. CONTROLLING OFFICE NAME AND ADDRESS U. S. Army Research Office P. O. Box 12211 Research Triangle Park, N. C. 27709		12. REPORT DATE (11) Dec [redacted]977 13. NUMBER OF PAGES 18
14. MONITORING AGENCY NAME & ADDRESS (*if different from Controlling Office*) (18) ARO (19) 12221.2-E		15. SECURITY CLASS. (*of this report*) Unclassified 15a. DECLASSIFICATION/DOWNGRADING SCHEDULE

16. DISTRIBUTION STATEMENT (*of this Report*)

Approved for public release; distribution unlimited

17. DISTRIBUTION STATEMENT (*of the abstract entered in Block 20, if different from Report*)

18. SUPPLEMENTARY NOTES

19. KEY WORDS (*Continue on reverse side if necessary and identify by block number*)

Viscous flows
Airfoil stall
Aerodynamics

20. ABSTRACT (*Continue on reverse side if necessary and identify by block number*)

The small separation bubbles which form near the leading edge of airfoils prior to the onset of leading-edge stall have been analyzed in detail, including the effects of viscous-inviscid interaction. The separated laminar shear layer, transitional flow and turbulent reattaching flow are represented [illegible] an integral formulation. A correlation of local shear-layer parameters has been developed for determining the onset

DD FORM 1 JAN 73 1473 EDITION OF 1 NOV 65 IS OBSOLETE

Unclassified 404 788

SECURITY CLASSIFICATION OF THIS PAGE (*When Data Entered*)

20. Cont'd

of transition in the laminar shear layer. Solutions are obtained using an iterative procedure, with strong interaction effects limited to the immediate vicinity of the separation bubble. Results obtained for specific airfoils are in good agreement with wind tunnel measurements. The method was used to investigate the mechanism for bubble bursting. Results indicate that reseparation of the turbulent boundary layer downstream of reattachment, rather than failure of the shear layer to reattach, causes bubble breakdown.

FOREWORD

This report was prepared by Avco Systems Division, Wilmington, Massachusetts, for the U. S. Army Research Office, Durham, North Carolina, in accordance with the requirements of Contract No. DAAG29-74-C-0035.

Dr. Peter Crimi was Principal Investigator for the reported study. Substantive contributions were made by Dr. Barry L. Reeves in the development of the viscous-flow representations.

Technical monitorship was provided by Dr. Robert E. Singleton of the U. S. Army Research Office.

CONTENTS

SUMMARY

The small separation bubbles which form near the leading edge of airfoils prior to the onset of leading-edge stall have been analyzed in detail, including the effects of viscous-inviscid interaction. The separated laminar shear layer, transitional flow and turbulent reattaching flow are represented by an integral formulation. A correlation of local shear-layer parameters has been developed for determining the onset of transition in the laminar shear layer. Solutions are obtained using an iterative procedure, with strong interaction effects limited to the immediate vicinity of the separation bubble. Results obtained for specific airfoils are in good agreement with wind tunnel measurements. The method was used to investigate the mechanism for bubble bursting. Results indicate that reseparation of the turbulent boundary layer downstream of reattachment, rather than failure of the shear layer to reattach, causes bubble breakdown.

1. INTRODUCTION

The regions of separated flow which form on airfoils govern the airfoil stall characteristics. The nature and extent of these regions are determined primarily by the airfoil shape, incidence and Reynolds number. Of concern here are the small separation bubbles which form near the leading edge of airfoils of moderate thickness ratio (.09 to .15) at chordal Reynolds numbers in the range from one to ten million. The occurrence of what is termed leading-edge stall, characterized by an abrupt loss in lift and increase in drag, can be attributed to the sudden breakdown, or bursting, of the leading edge bubble (Reference 1).

The flow in the vicinity of the leading edge of an airfoil subject to leading-edge stall is as sketched in Figure 1. The laminar boundary layer, extending from the stagnation point over the leading edge, separates just downstream of the point of minimum pressure. Transition to turbulent flow occurs in the free shear layer a short distance downstream of the separation point. The flow then reattaches to the airfoil surface, with a turbulent boundary layer extending from the reattachment point to the trailing edge. If the angle of attack of the airfoil is increased, the bubble moves closer to the leading edge and becomes slightly shorter. The bubble has almost no effect on integrated loads, because it is never more than a few percent of the chord in length. In the immediate vicinity of the bubble, though, there is strong interaction between the viscous and inviscid flows.

The specific mechanism for bubble breakdown is not presently known. It has been postulated, though, that there is a physical limitation in the amount of pressure recovery possible in the turbulent shear layer, so the bubble bursts when the limit is exceeded and the shear layer fails to reattach. Alternatively, it has been suggested that stall results from separation of the turbulent boundary layer just downstream of reattachment (Reference 2). This study was undertaken to provide a tool for investigating the specific mechanism for breakdown of the leading-edge bubble and, ultimately, for accurately predicting the onset of leading-edge stall.

Leading-edge bubbles have been the subject of numerous studies. Reviews of this work are given in References 2 and 3. The primary difficulties in treating the problem analytically derive from the interaction between the viscous and inviscid flows and

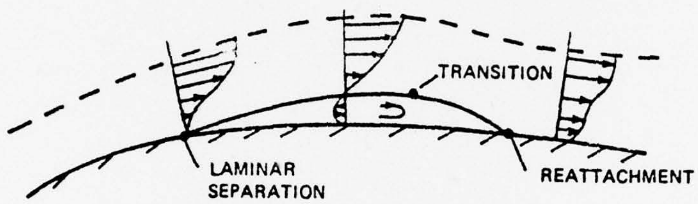

Figure 1 FLOW IN THE VICINITY OF A LEADING-EDGE BUBBLE

the coupling between the interaction and transition from laminar to turbulent flow in the free shear layer. Analyses have been carried out using semi-empirical formulations which do provide fairly good qualitative agreement with tests in predicting stall onset (References 4 and 5). However, the modeling has not been adequate for analyzing the details of the flow in and near the bubble.

More recently, separation bubbles which occur near midchord on relatively thick airfoils at zero incidence were analyzed numerically using a finite-difference method (Reference 6). While these bubbles are about ten times longer than leading-edge bubbles, their structure is quite similar, with transition occurring in the free shear layer. The results of that analysis are in excellent agreement with the flow measurements reported in Reference 7. It should be noted, in particular, that in Reference 6 interaction was assumed to be limited to the vicinity of the bubble. Also, the validity of the boundary-layer approximation for analyzing the bubble was verified by direct comparison with a solution using the complete Navier-Stokes equations.

In this study, the separated and reattaching shear layer in a leading-edge bubble were analyzed using an integral formulation, assuming the boundary-layer approximation is applicable. Interaction between the viscous and invescid flows in the vicinity of the bubble was taken into account through an iterative procedure. The method of analysis is outlined briefly in the next section. Derivation of the formulations employed and results of analyses for different airfoil sections, angles of attack and Reynolds numbers are presented in Reference 8.

The method developed for analyzing leading edge bubbles was employed to investigate the specific mechanism for bubble burst. Details of that analysis are given in Section 3.

2. METHOD OF ANALYSIS OF LEADING-EDGE BUBBLES

Inviscid Flow Representation

Assuming the flow to be two-dimensional, let $u_o(x)$ denote the magnitude of fluid velocity at the airfoil surface that would result in the absence of viscous effects, where x is a co-ordinate measured along the airfoil surface. The flow component tangent to the airfoil surface at the interface of the viscous and inviscid flows is written in the form

$$u_e(x) = u_o(x) \left[1 + \tilde{u}(x) \right] \quad (1)$$

A previously developed digital computer program is employed in the analysis to direct the computation of u_o, given the airfoil shape and angle of attack, using a source distribution on the airfoil surface and a vortex distribution on the chord line.

The analyses of the boundary layer and shear layer provide the flow inclination v_e/u_e at the interface of the viscous and inviscid flows, which can be related to $\tilde{u}$ as follows. Interaction is taken to occur on the interval $x_A \leq x \leq x_B$, over which it is assumed the surface curvature is negligible. The perturbation to the inviscid flow is derived from a potential; the potential is formulated from a source distribution on the airfoil surface.

With $m(x) \equiv v_e/u_e \approx v_e/u_o$, and assuming $\tilde{u} \ll 1$, it is found that

$$\tilde{u}(x) = \frac{1}{\pi} \int_{x_A}^{x_B} \frac{m(\xi)\, d\xi}{x - \xi} \quad (2)$$

Viscous Flow Representation

The flow in the free shear layer and the boundary layer in the vicinity of the separation bubble are represented using the integral formulation developed in Reference 9 for analyzing supersonic separated and reattaching laminar flows involving strong interaction with the inviscid flow. The relations have been generalized to account for continuous transition from laminar to turbulent flow in the free shear layer. Both the momentum integral (zeroth moment) and first moment of momentum of the boundary layer equations are used, so that for laminar or fully turbulent flow the velocity profiles can be characterized by a single parameter which is not related to the local pressure gradient. The family of similar solutions for reversed flow found by Stewartson (Reference 10) is employed for analyzing the free shear layer. Turbulence production is introduced using an exponentially increasing intermittancy function, with the constant in the exponent determined from measurements taken in a free shear layer undergoing transition (Reference 11).

A coupled pair of first-order, ordinary nonlinear differential equations was derived from the momentum equations. They have been formulated in such a way that they can be integrated continously downstream, starting in the laminar boundary layer and continuing through the separation point, transition in the laminar shear layer and reattachment of the turbulent shear layer. The dependent variables are the displacement thickness δ^* and a parameter, denoted a, characterizing the velocity profile. That parameter is defined as follows:

$$a = \frac{\delta}{u_e} \left(\frac{\partial u}{\partial y}\right)_{y = 0} \text{, attached flow;} \tag{3a}$$

$$a = \left(\frac{y}{\delta}\right)_{u = 0} \text{, separated flow.} \tag{3b}$$

The integral across the boundary layer of the momentum equation and of that equation multiplied by u then give, under the aforementioned assumptions, a pair of differential equations of the form

$$\frac{d\,\delta^*}{dx} = (f_{\delta^*} + g_{\delta^*} u_e') / u_e + h_{\delta^*} \tag{4}$$

$$\frac{da}{dx} = (f_a + g_a u_e') / u_e + h_a \tag{5}$$

where the f's, g's and h's are nonlinear functions of δ^* and a. With $u_e(x)$ specified, Eqs. (4) and (5) can be integrated numerically on x to obtain δ^* and a.

To complete the basic formulation of the viscous flow, the continuity equation provides the following relation for flow inclination at the edge of the layer:

$$m(x) \equiv v_e/u_e = \frac{d\delta^*}{dx} - Z \frac{\delta^*}{u_e} \frac{du_e}{dx} \tag{6}$$

where $$Z = \frac{1}{\delta^*} \int_0^{\delta} \frac{u}{u_e} \, dy$$

This equation forms part of the link between the viscous and inviscid flow solutions in the iteration, as discussed subsequently.

Transition Onset

A relation of the form

$$\left(\frac{u_e \delta^*}{\nu} \right)_s = f \left(\frac{a_t \; \delta_t}{\delta_s^*} \right)$$

was postulated for correlating transition onset location in the bubble, where subscripts s and t refer to separation and transition onset, respectively. Using the measured pressure distributions given in Reference 7, Eqs. (4) and (5) were integrated through separation and into the laminar free shear layer to provide streamwise variations of a δ . A total of 15 cases were analyzed, including leading-edge bubbles on two different airfoils, each at two different angles of attack, for free-stream Reynolds numbers ranging from 1.5 x 10^6 to 6 x 10^6. For each case, the measured location of transition given in Reference 7 was used to obtain the appropriate value of $a_t \, \delta_t/\delta_s^*$. The results obtained are plotted in Figure 2. While there is some scatter, particularly at the higher Reynolds numbers, the data are still well correlated by the postulated relation. The line drawn through the points is a plot of the simple relation

$$\frac{a_t \, \delta_t}{\delta_s^*} = \frac{10^6}{\left(\frac{u_e \, \delta^*}{\nu} \right)_s^2}$$

which is seen to provide a quite good approximation to the derived correlation. This equation was used in the bubble analyses to locate transition onset.

Iteration Procedure

An iteration step is begun by integrating Eqs. (4) and (5) to obtain δ^* and a as a function of x, given u_e and u_e'. The step is completed by obtaining revised estimates of u_e and u_e' as dictated by the relations governing the viscous-inviscid

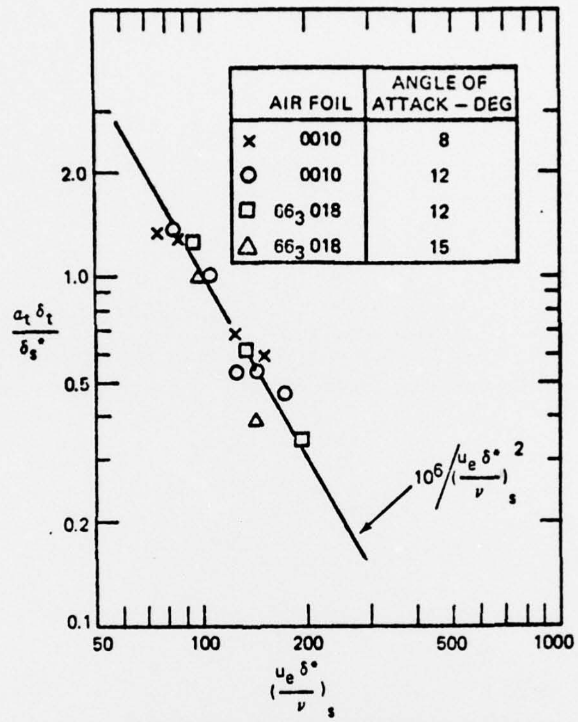

CORRELATION OF SHEAR LAYER PARAMETERS AT TRANSITION ONSET IN A LEADING-EDGE BUBBLE

FIGURE 2

interaction. The obvious procedure of simply substituting the variation of v_e/u_e obtained from the viscous-flow analysis, Eq. (6), into the integrand of Eq. (2), was found to be unsuitable. The initial estimate for the u_e variation inevitably produces small but physically unrealistic excursions in δ^* in the immediate vicinity of transition which cause rapid divergence of results for successive iterations. The following procedure was therefore devised.

The interaction is introduced using the differential equation for δ^*, Eq. (4), as a link to the variation of δ^* obtained in the analysis of the viscous flow. Specifically, a and δ^*, and hence the coefficients f_{δ^*}, f_a, etc., are regarded as known in Eq. (4), their variation having been determined from the viscous-flow analysis, while $d\delta^*/dx$, du_e/dx, and u_e are regarded as unknown. By combining Eqs. (1), (2) and (6) in Eq. (4), one then obtains a linear integro-differential equation for the flow inclination m(x). This equation is solved using techniques analogous to those employed in thin-airfoil theory. A weighted average of the previous and derived variations of u_e is then employed to begin the next iteration step.

Representative Results

Results of a bubble analysis for the case of a modified NACA 0010 airfoil at 8 degrees angle of attack and chordal Reynolds number of 2×10^6 are shown in Figure 3, where variations between separation and reattachment of u_e, δ, δ^* and the ordinate where u = 0 are plotted. The agreement between computed and measured variations of u_e and the locations of reattachment (measured location is marked by a small arrow on the abscissa) are seen to be very good. Further results are given in Reference 8.

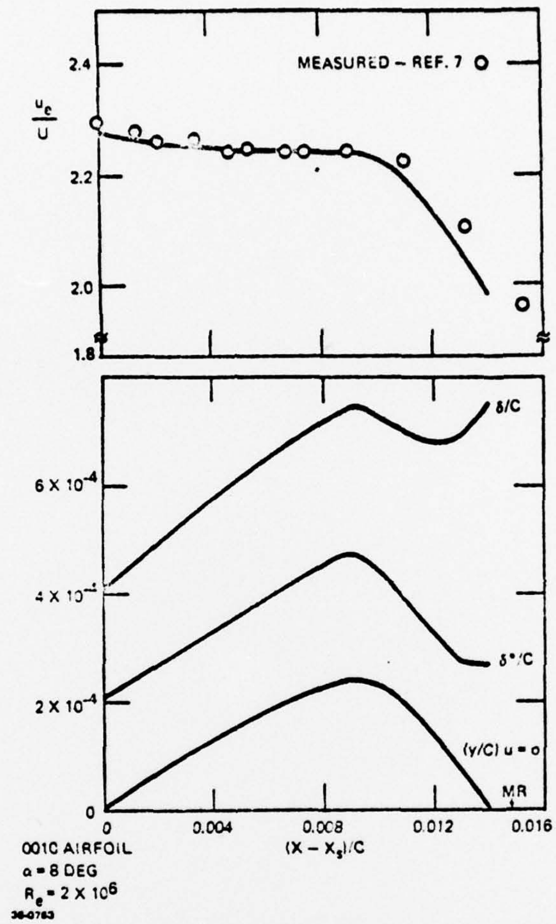

Figure 3 RESULTS OF LEADING-EDGE BUBBLE ANALYSIS FOR A 0010 AIRFOIL IN INCOMPRESSIBLE FLOW; α = 8 DEG, $Re = 2 \times 10^6$

3. ANALYSIS OF BUBBLE BURST MECHANISM

An analysis was undertaken, using the method outlined in the previous section as the basic tool, with the aim of determining whether bubble burst can be attributed to either failure of the shear layer to reattach or to reseparation downstream of reattachment. The NACA 0012 airfoil section, which is generally accepted as being subject to leading-edge stall, and for which there is a large body of data concerning stall available, was selected as the specific subject for analysis.

As a first step, the potential flow and loading for incipient stall was defined. Data on maximum lift coefficient $C_{\ell\,max}$ was obtained from References 12 through 15, and the plot of $C_{\ell\,max}$ vs. chordal Reynolds number shown in Figure 4 was generated. A Reynolds number of 2×10^6 was selected for detailed analysis, as that value is well within the Reynolds number range over which leading-edge stall takes place (roughly 10^6 to 6×10^6 - see Reference 2). From Figure 4, it is seen that at this Reynolds number bubble burst should occur at a lift coefficient of 1.37.

Addressing first the question of whether burst is due to failure to reattach, analyses of leading-edge bubbles on a 0012 airfoil at a Reynolds number of 2×10^6 were carried out using the procedures described in the previous section, for lift coefficients of 1.27 (i.e., somewhat below stall), 1.37 (incipient stall), and 1.57 (well above stall). The nominal potential flow for an unstalled airfoil was used in all three cases. Results obtained are shown in Figure 5, where the variations between separation and reattachment of u_e, δ, δ^* and the ordinate where $u = 0$ are compared.

It should be noted, first, that converged solutions were obtained for all three cases without difficulty. The case with C_ℓ equal to 1.57 does exhibit a tendency for failure to reattach, in that near reattachment the slope of the ordinate where $u = 0$ is about half of what was obtained with lower values of C_ℓ. Nevertheless, a converged solution was obtained with a loading about 11 percent greater than that required to cause bubble burst, strongly suggesting that failure to reattach is not the burst mechanism.

Next, an attempt was made to determine directly whether bubble burst is due to reseparation of the turbulent boundary layer just downstream of reattachment, where strong interaction between

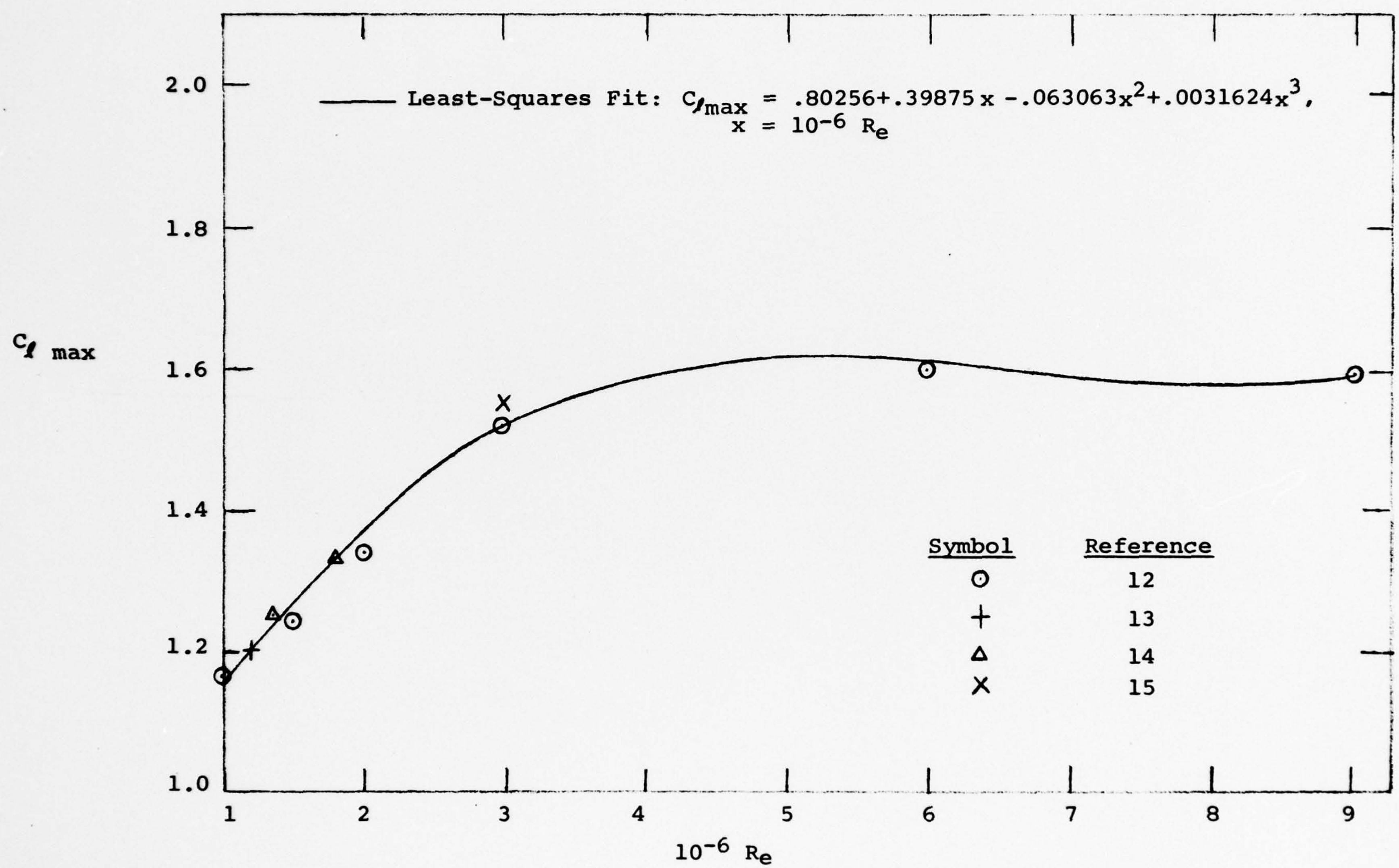

Figure 4 - Variation of maximum lift coefficient with Reynolds number for the NACA 0012 airfoil section.

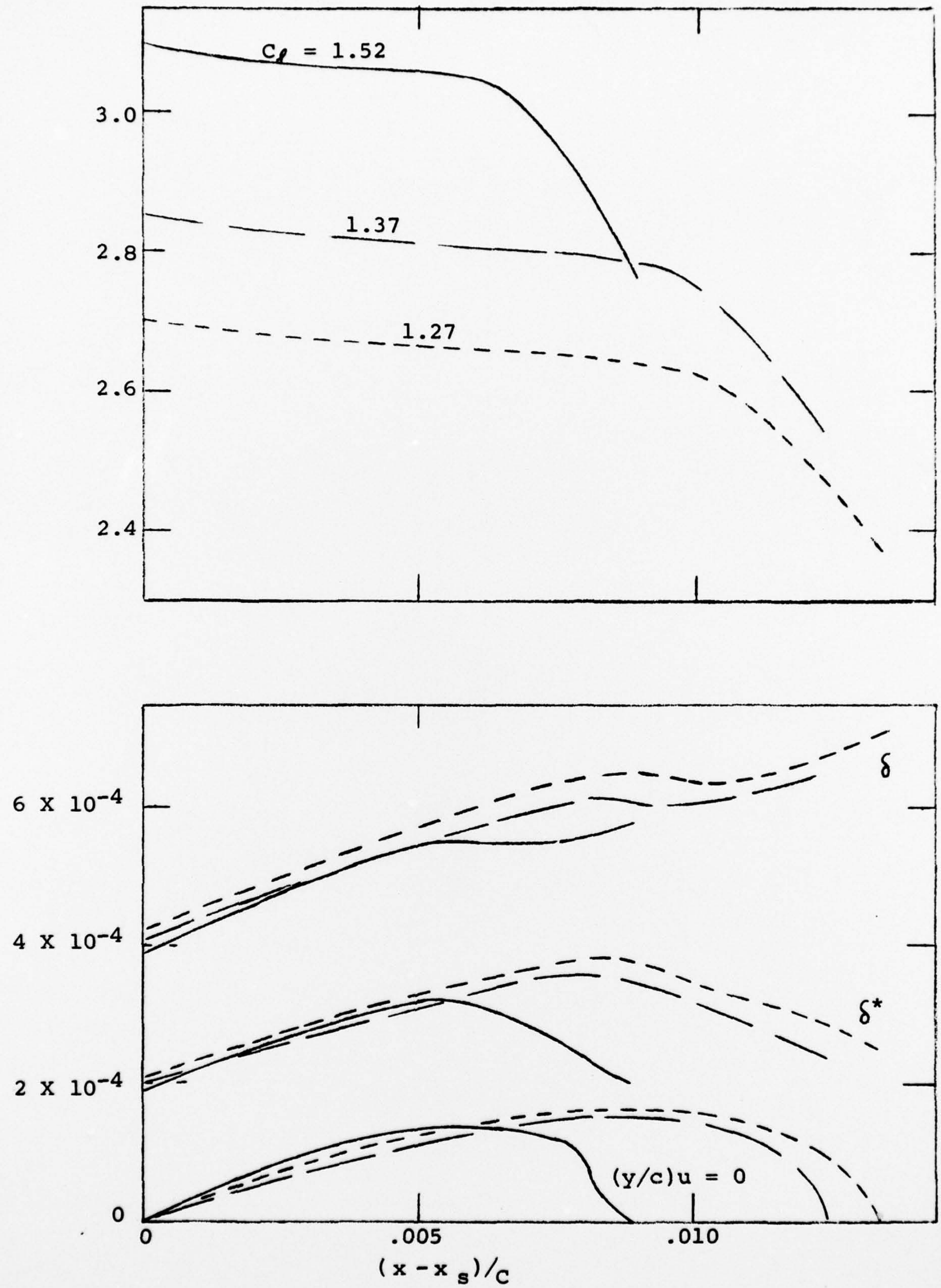

Figure 5 - Comparison of results of bubble analyses for three different lift coefficients, 0012 airfoil, $R_e = 2 \times 10^6$.

the viscous and inviscid flows must still be taking place. The formulations employed to analyze the bubble shear layers could not be used directly to analyze the turbulent boundary layer, because the turbulent wall shear is not properly taken into account in those relations.

To represent the turbulent boundary layer, it was first decided to employ the finite-difference method of Reference 5 and perform a direct iteration between viscous and inviscid flows downstream of reattachment, while retaining the indirect iteration procedure for the bubble. The finite-difference turbulent boundary layer code was successfully incorporated in the bubble analysis program. A displacement thickness variation downstream of reattachment was then obtained from an initial estimate of the u_e variation there, for an airfoil loading somewhat below stall. Attempts to iterate were then made, but unfortunately the solutions were strongly divergent, the difficulty apparently stemming from extreme sensitivity of the solution to the pressure gradient just downstream of reattachment.

It was then decided to abandon the finite-difference approach and instead use an integral formulation and an iterative procedure analogous to the one used for the bubble itself. The integral relations developed for the turbulent boundary layer are outlined in the Appendix. These relations were successfully incorporated in the bubble analysis code, and again a solution was obtained for the boundary layer downstream of reattachment for an initial assumed pressure distribution. An iterative procedure was then set up which is exactly analogous to the one used for the bubble. That is, the differential equation for δ^* was used to generate a linear integro-differential equation for the flow perturbation. This equation was solved in exactly the same manner as for the bubble, again using a trigonometric series to represent the flow perturbation. Unfortunately, this approach was not successful either, the solution for the flow after the first iteration being completely unrealistic. The cause of the difficulty is not presently clear. A simple error in the formulations or coding cannot be ruled out, but the equations and program were carefully checked. Another possibility is the method used to integrate through the singularity just downstream of reattachment. The same procedures as were used in the bubble analysis were employed for that singularity. The solution appears to depend strongly on the gradient in δ^* at the singularity obtained by these procedures. It may be that the boundary-layer equations are sufficiently different from those of the shear layer that a revised approach is required to integrate through the singularity.

It does appear, since the bubble analysis was successful, that a solution for the turbulent boundary layer in the vicinity of reattachment can be obtained using an integral formulation and an indirect iteration procedure. Unfortunately, the limitations in the scope of this study precluded further pursuit of that approach.

It can be tentatively concluded, in any case, that the specific mechanism for bubble burst is not failure to reattach, but rather must involve the downstream turbulent boundary layer. Further analysis should be directed first to accurately defining the flow in the boundary layer just downstream of reattachment, taking strong interaction effects into account.

4. REFERENCES

1. McCullough, G. B., and Gault, D. E., "Examples of Three Representative Types of Airfoil-Section Stall at Low Speed," NACA TN 2502, September 1951.

2. Ward, J. W., "The Behavior and Effects of Laminar Separation Bubbles on Aero-Foils in Incompressible Flow," J. Roy. Aero. Soc., Vol. 67, December 1963.

3. Tani, I., "Low-Speed Flows Involving Bubble Separations," Prog. in Aero. Sci., Vol. 5, Pergamon Press, 1964, pp. 70-103.

4. Horton, H. P., "A Semi-Empirical Theory for the Growth and Bursting of Laminar Separation Bubbles," ARC CP No. 107, June 1967.

5. Crimi, P., and Reeves, B. L., "A Method for Analyzing Dynamic Stall of Helicopter Rotor Blades," NASA CR 2009, May 1972.

6. Briley, W. R. and McDonald, H., "Numerical Prediction of Incompressible Separation Bubbles," J. Fluid Mech., Vol. 69, Part 4, June 1975, pp. 631-656.

7. Gault, D. E., "An Experimental Investigation of Regions of Separated Laminar Flow," NACA TN 3505, September 1955.

8. Crimi, P., and Reeves, B. L., "Analysis of Leading-Edge Separation Bubbles on Airfoils," AIAA J., Vol. 14, No. 11, November 1976.

9. Lees, L., and Reeves, B. L., "Supersonic Separated and Reattaching Laminar Flows: I. General Theory and Application to Adiabatic Boundary-Layer/Shock-Wave Interactions," AIAA J., Vol. 2, No. 11, November 1964, pp. 1907-1920.

10. Stewartson, K. "Further Solutions of the Falkner-Skan Equation," Proc. Cambridge Phil. Soc., Vol. 50, Part 3, July 1954.

11. Ojha, S. K., "An Experimental Study of Laminar Separation Bubbles," Indian Institute of Technology, Rept. No. AE186/A, April 1967.

12. Loftin, L. and Smith, H., "Aerodynamic Characteristics of 15 Airfoil Sections at Seven Reynolds Numbers from .7 x 10^6 + 9.0 x 10^6," NACA TN 1945, October 1949.

13. Lizak, A., "Two-Dimensional Wind Tunnel Tests of an H-34 Main Rotor Airfoil Section," TREC Tech. Rept. 60-53, September 1960.

14. Critzos, C., Heyson, H., and Boswinkle, R., "Aerodynamic Characteristics of NACA 0012 Airfoil Section at Angles of Attack from 0^o to 180^o," NACA TN 3361, January 1955.

15. Martin. J., Empey, R., McCroskey, W., and Caradonna, F., "A Experimental Analysis of Dynamic Stall on an Oscillating Airfoil," <u>J. Am. Helicopter Soc.</u>, Vol. 19, No. 1, January 1974, pp. 26-32.

16. Coles, D. E. and Hirst, E. A. (Eds.), "Proceedings of AFOSR-IFP-Stanford Conference on Computation of Turbulent Boundary Layers," August 1967.

APPENDIX

Relations for Analyzing the Turbulent Boundary Layer

The procedure for analyzing the turbulent boundary layer was developed to provide an analytic form which is compatible with the relations used for the shear layer. Specifically, a pair of ordinary first-order differential equations, with δ^* and a profile parameter as dependent variables, was derived.

Starting from the momentum integral and first moment equations, it was decided to employ the same basic approach as that of Albers (Reference 16) whereby the equations are partially decoupled from the local pressure gradient, except for two departures from Albers' approach. Specifically, rather than evaluate dH/dx and dJ/dx separately, it is assumed that dJ/dx = (dJ/dH)(dH/dx), where dJ/dH is a function of profile parameter a and the friction coefficient C_f. Also, a relation for C_f was adopted which closely approximates that of the Ludwieg-Tillman correlation (Reference 16) near separation, namely

$$C_f = .041\ a\ R_{e_\Theta}^{-.268}$$

where the profile parameter a is defined by

$$a \equiv \frac{H}{H_s} -1 = \frac{H}{.429} -1$$

and R_{e_Θ} is local momentum - thickness Reynolds number.

The specific relations derived are then as follows.

$$\frac{d\delta^*}{dx} = \frac{1}{(HdJ/dH-J)}\left\{ f^2 dJ/dH-D+ \left[3J-(2H+1)dJ/dH\right] \frac{\delta^*}{u_e} du_e/dx \right\}$$

$$\frac{da}{dx} = \frac{2.332}{\delta^*(HdJ/dH-J)}\left\{ HD-f^2J+J(1-H) \frac{\delta^*}{u_e} du_e/dx \right\}$$

where $f^2 = C_f/2$

$$H = .429(a+1)$$

$$J = 3H-1+I_3/I_1$$

$$dJ/dH = 3\left[1-(1.7f+1.2994\mu)/K\right]$$

$$D = \frac{\left[KJI_1 - f(2I_3 - 3I_2)\right]\left[f^2 + (1 + H)\beta\right]}{KHI_1 + f\ I_2} - 2J\beta$$

$$K = .41$$

$$\beta = \beta_1 \quad \text{if} \quad \beta_1 \geqq 0$$

$$\beta = \beta_2 \quad \text{if} \quad \beta_1 < 0$$

$$\beta_1 = \left[(1 - H + 1.5\ f)/6.231\right]^2 - 1.81\ f^2$$

$$\beta_2 = f\left[1 - H - 6.883\ f\right]$$

$$I_1 = (f + \mu)/K$$

$$I_2 = 2(f^2 + 1.59\ f\mu + .74812\mu^2)/K^2$$

$$I_3 = 6(f^3 + 1.84\ f^2\mu + 1.57\ f\mu^2 + .42\mu^3)/K^3$$

$$\mu = \left\{\left[\lambda^2 - 2.9925\ f(\lambda - .59\ f)\right]^{1/2} - \lambda\right\}/1.4962$$

$$\lambda = 1.59\ f + .205\ (H - 1)$$